Electronic Supplementary Material (ESI) for Environmental Science: Nano.

Role of NOM-Hematite Nanoparticle Complexes and Organic and Inorganic Cations in the Coherence of Silica and Clay Particles: Evaluation based on Nanoscale Forces and Molecular Self-assembly

Zhenquan Wang[a], Bo Feng[b], Di Zhang[a], Saikat Ghosh[a]* Bo Pan[a], Baoshan Xing[c]

[a]Kunming University of Science and Technology, Kunming, China

[b]Chongqing Key Laboratory of Soil Multi-Scale Interfacial Processes, College of Resources and Environment, Southwest University, Chongqing 400715, China

[c]Stockbridge School of Agriculture, University of Massachusetts, Amherst, Massachusetts 01003, United States

*Corresponding Author's E-mail: sghosh12@qq.com (Saikat Ghosh)

Phone: +86-158-8708-5160

Table S1. Elemental Composition of HA.[1]

	%C	%O	%H	%N
HA	54.1	39.3	4.3	2.3

Table S2. Molecular weight of HA.

Mp	Mn	Mw	Mz	Mz+1	Mv	PD
785	872	1508	2504	3612	1387	1.72936

Evaluation of hematite NPs XRD: The XRD pattern of the 7 nm Hematite NPs synthesized by us has matched closely with the standard literature database. Nearly same-sized hematite NPs were synthesized

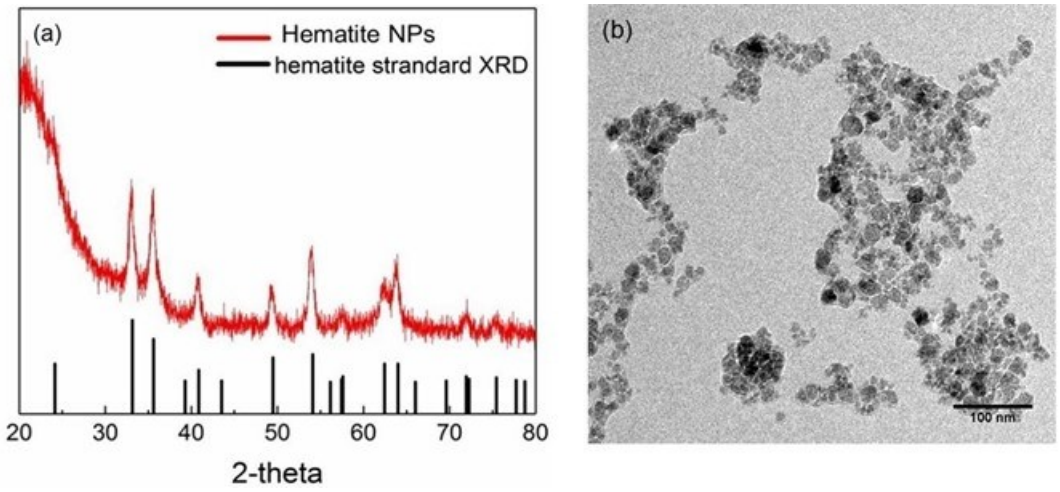

Figure S1. (a) X-ray diffraction pattern of hematite NPs and the standard obtained from the Jade pdf database. (b) TEM image of the hematite NPs at pH 6.

earlier by Prof. Michael Hochella's group at Virginia Tech., and we have followed the same procedure regarding hematite synthesis. We compared the diffraction peaks of the hematite NPs synthesized by us with the XRD data of size variant hematite NPs having average diameters of 7 nm, 25 nm, and 88 nm, synthesized by Madden et al. (2007).[2] The diffractions peaks of 7 nm

hematite synthesized by us match with the XRD pattern of the 7nm hematite synthesized by Madden et al. (2007).[2] Except matching of the XRD peaks both the diffraction patterns have a high background. In both, the particle reduction in particle size contributed to the loss of crystalline along with the rise in crystal defects.

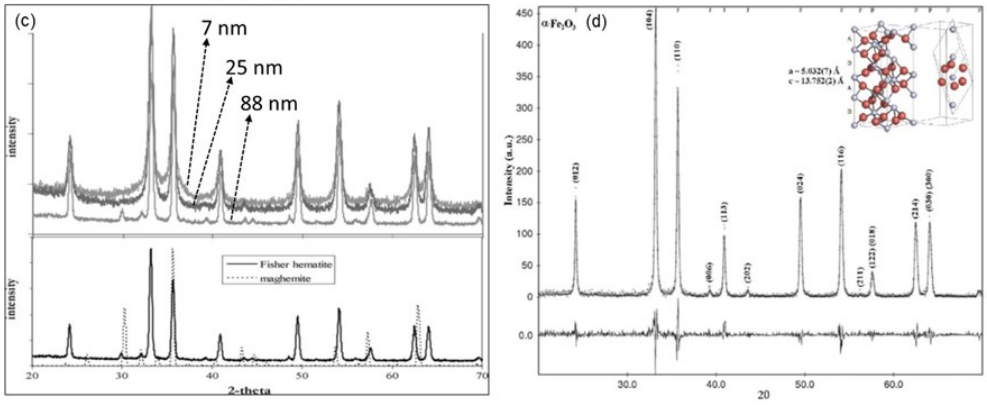

XRD data of 7 nm, 25 nm, and 88 nm hematite NPs (synthesized by Madden et al., 2003) and XRD peaks of 50 nm hematite NPs synthesized by Xu et al. (2015).

Moreover, XRD peaks of 50 nm hematite NPs synthesized by Habib et al. (2015) (figure 1d) match more closely with the 88 nm diameter sized hematite nanocrystals synthesized by Madden et al. (2007).[2-3] Our previous work on two different aspect ratio goethite nanocrystals also revealed that the high aspect ratio goethite NPs has higher crystal defects (Ghosh et al., 2016).[4] In addition, magnetization measurements elucidated loss of antiferromagnetic order contributed to the magnetic properties in the high-aspect ratio goethite NPs.[4]

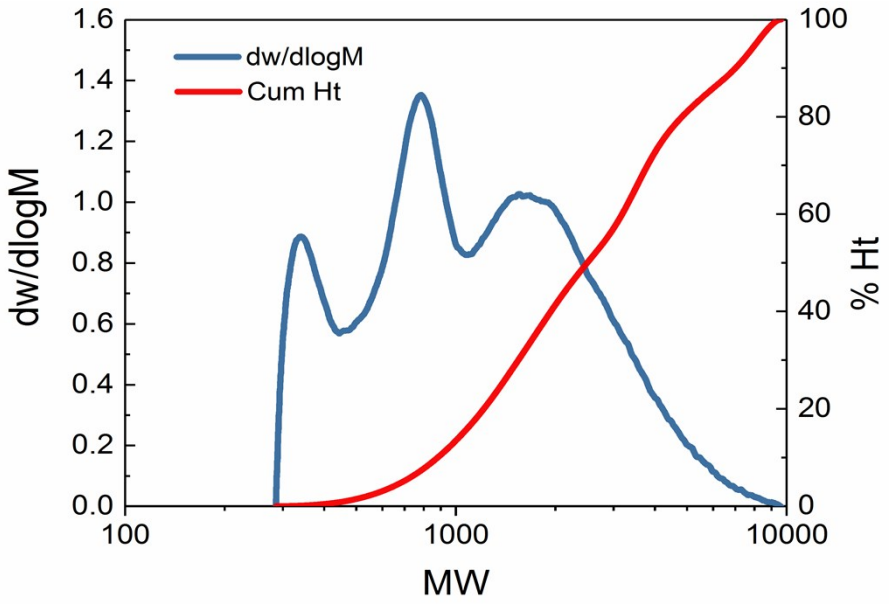

Figure S2. Molecular weight of HA determined by GPC.

Molecular Weight (MW) of HA

The molecular weight of HA was determined by gel permeation chromatography (GPC). Briefly, 100 µL of 100 mg/L HA solution was filtered through a 0.45 µm polycarbonate membrane filter and then injected into a PL-GPC 50 GPC system (Agilent, USA) equipped with an Agilent PL aquagel-OH column (300 x 7.5 mm) and a refractive index (RI) detector. A 2 mM phosphate buffer solution maintained at pH 6.0 was used as a mobile phase with a 1 mL/min flow rate. Polyethylene glycol (PEG) and polyethylene oxide (PEO) with MWs of 162, 580, 1260, 3370, 450, 19720, 60450, 184900, 483000, 915000, 3053000, and 6035000 D (Agilent, U.S.A.) were used as standards to determine the HA molecular weight, a required parameter for ITC calculations.

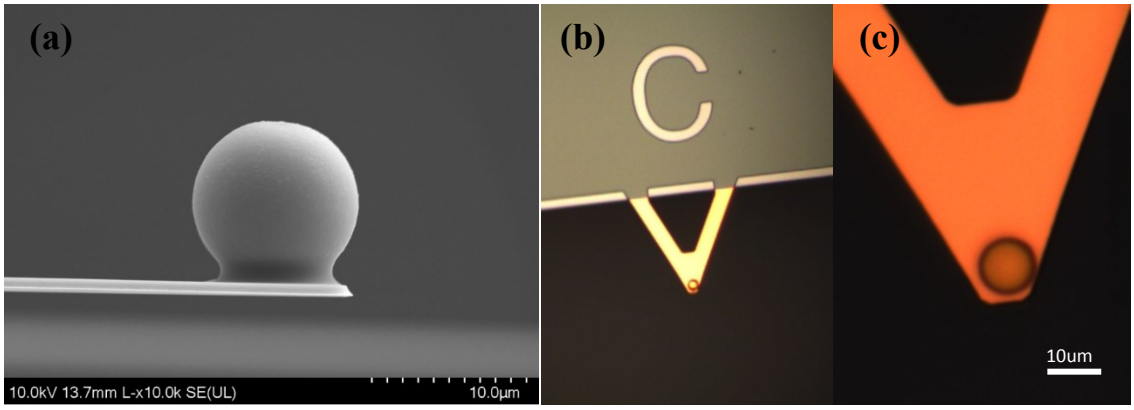

Figure S3. (a) scanning electron microscopy (SEM) and (b and c) optical microscopy images of the bare silica probes**.**

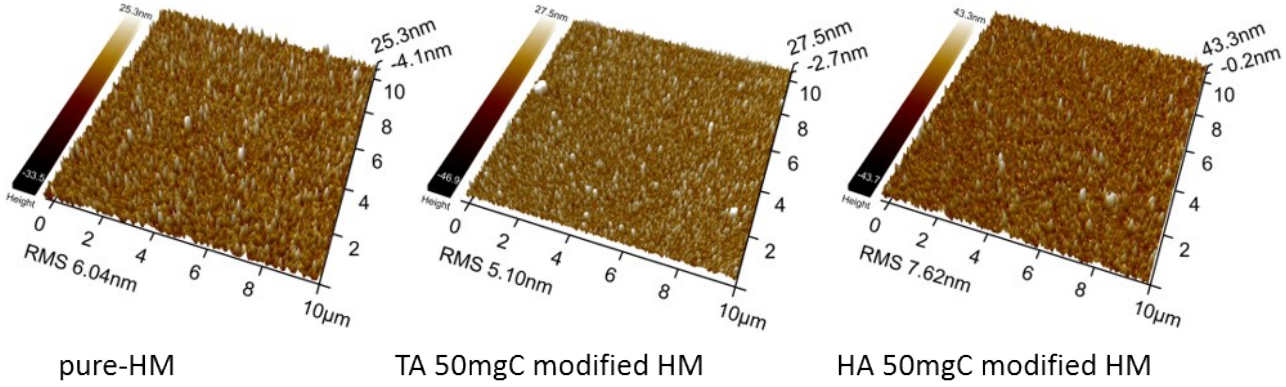

Figure S4. 3D-AFM images of the hematite-coated mica (Hm-mica) and HA- and TA-modified Hm-mica substrates with root mean square (RMS) roughness of 6.0 nm, 5.1 nm, and 7.6 nm respectively.

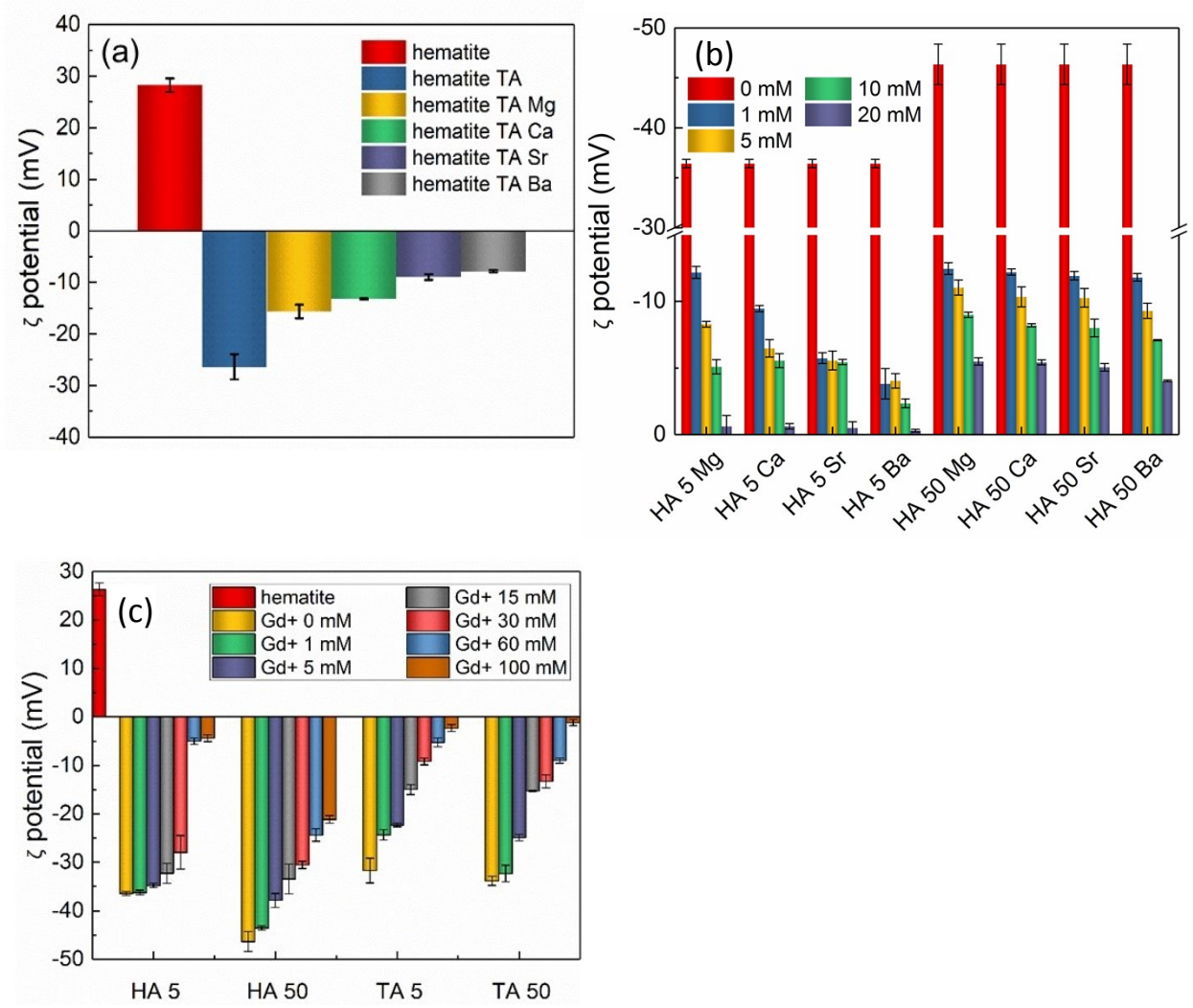

Figure S5. (a) ζ-potential data of hematite NPs (5 mg/L) and TA (5 mg C/L) mixture in the presence of inorganic cations at pH 6. (b) ζ-potential data of the mixtures of hematite NPs (5 mg/L) HA at pH 6 and in the presence of 0, 1, 5, 10, 20 mM salts. HA 5 and HA 50 represent 5 mg C/L, and 50 mg C/L concentrations of HA. The addition of inorganic cations reduced the magnitude of ζ. The lowest |ζ| was recorded for Ba^{2+}. (c) ζ-potential data of hematite NPs-HA and hematite NPs-TA mixtures in the presence of Gd^{+} at pH 6. HA 5 and HA 50, and TA 5 and TA50 represent 5 and 50 mg C/L concentrations of the NOMs.

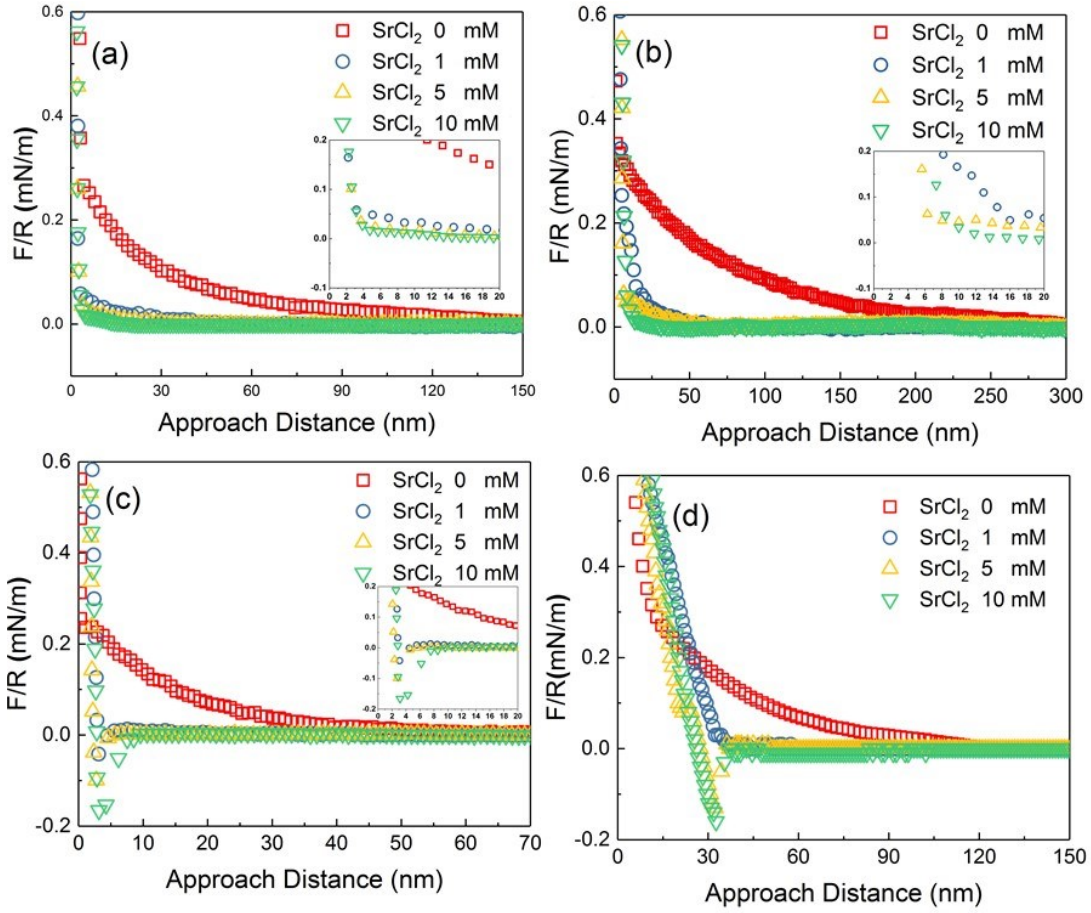

Figure S6. F/R vs D approach curves of the silica probe with (a) 5 mg C/L and (b) 50 mg C/L HA-modified Hm-mica in the presence of Sr^{2+}. The salt concentrations ranged between 0-10 mM. The inset images show the lower limits of the approach curves. F/R vs D approach curves of the silica probe with Hm-mica in (c) 5 mg C/L and (d) 50 mg C/L TA within 0-10 mM Sr^{2+}.

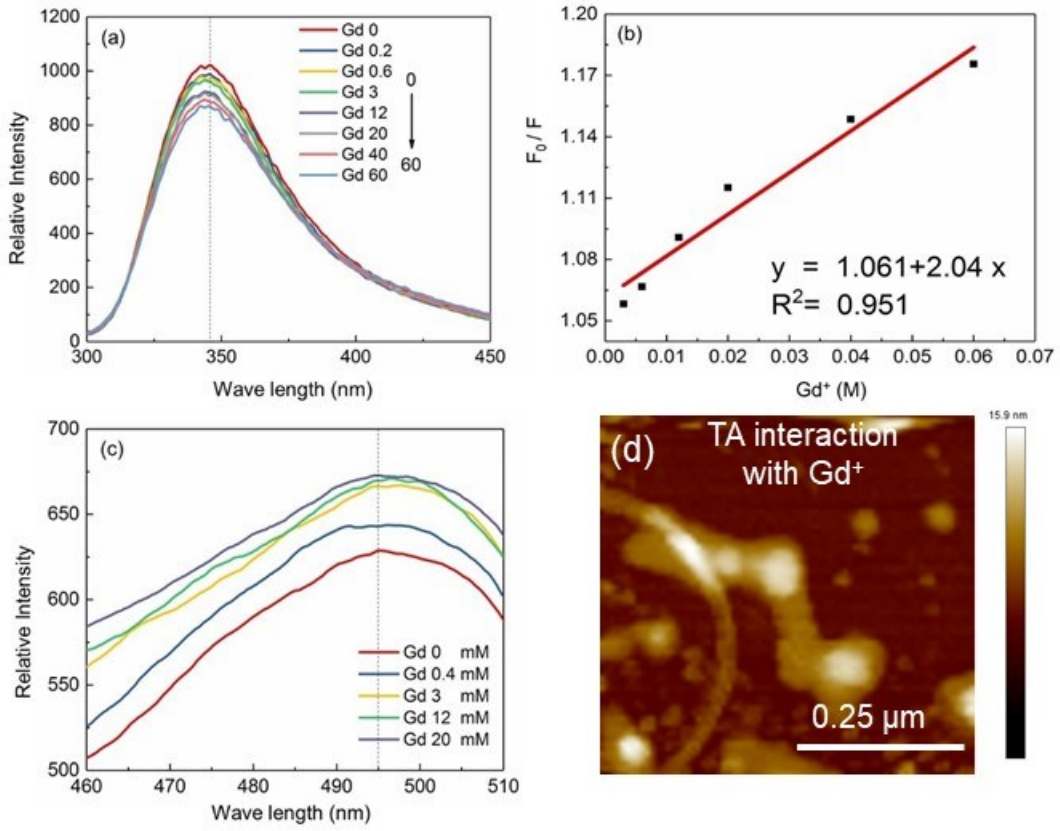

Figure S7. Fluorescence titration experiments of (a) TA with Gd^+ showed fluorescence quenching with increasing Gd^+ concentrations and the corresponding (b) Stern-Volmer plot reflects static quenching, which attributed to cation-π interactions. Fluorescence titration experiment of (c) HA and Gd^+ showed trivial enhancement in fluorescence quantum yield against dissipative loss. (d) TA interaction with Gd^+ and the growth of amphiphilic helical aggregates due to molecular gelation and likely formation of H-aggregates.

According to McRae and Kasha side-by-side arrangement of transition dipoles facilitated positive Coulomb coupling between the molecules and facilitate H-aggregates formation, and resulted in the development of singlet state bands (excitons). The higher energy state of the excitons consumes all of the oscillator strength along with "Fluorescence suppression and favored strong intersystem crossing and Phosphorescence" (Kashas's Rule) as described by Hestand and Spano (2018).[6-7] In contrast, "head-to-tail" alignment of transition dipoles and

negative Coulomb coupling produce J-aggregates. The oscillator strength is focused on the lowest energy excitons with minimal fluorescence suppression. The detailed electronic coupling method was described by Heyene (2016).[8] Apparently, Gd^{+} interactions with HA and movement of the fluorescence emission spectra to a higher wavelength is a characteristic of J-type aggregates, with the head-to-tail alignment of transition dipoles based on Kasha's rule. Considering the complexity of HA and the diversity of fluorophores, separate investigations are required.

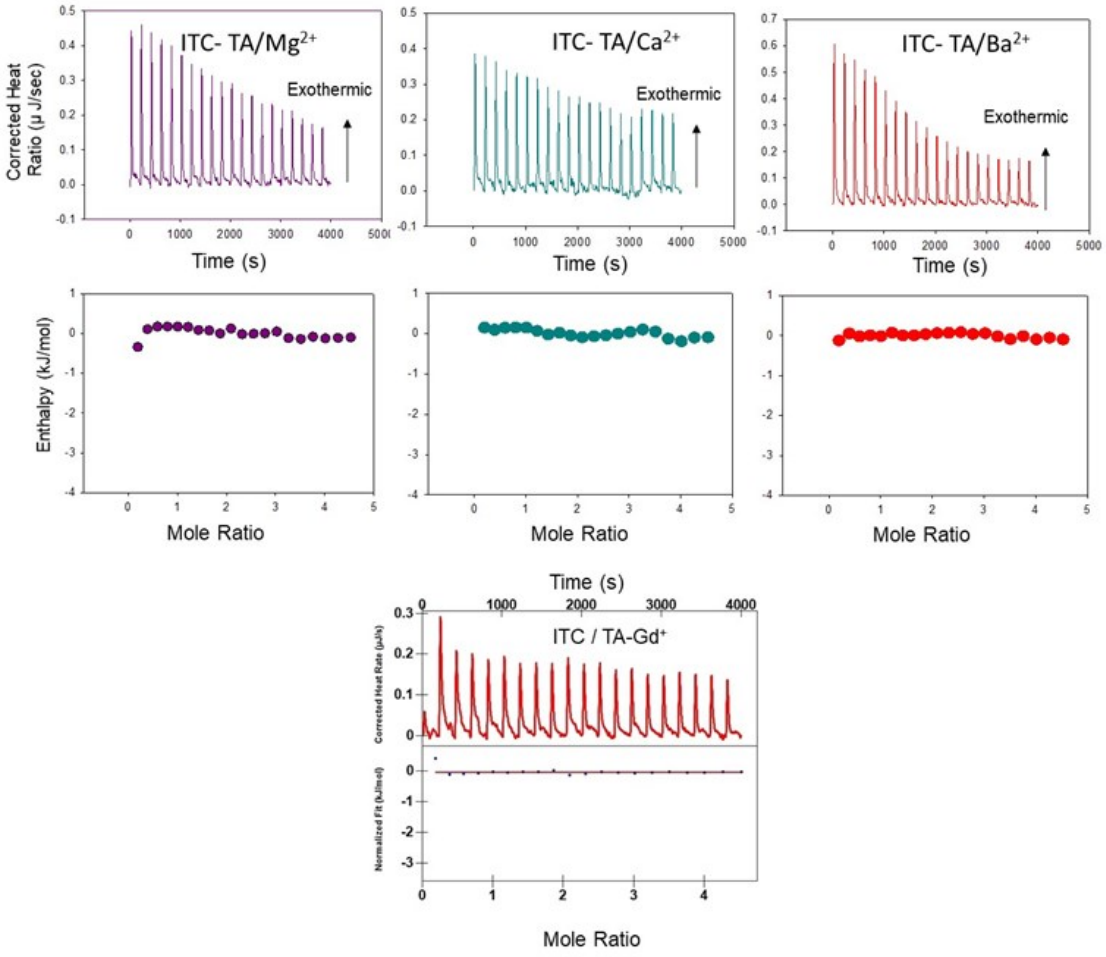

Figure S8. ITC data of TA (a) with Mg^{2+}, Ca^{2+}, Ba^{2+} and Gd^{+} at pH 6. Unlike HA interactions with Ba^{2+} and Gd^{+} reduced ionization of TA at pH 6 showed weaker interaction energy or enthalpy change.

References

1. X. Wang, L. Shu, Y. Wang, B. Xu, Y. Bai, S. Tao and B. Xing, Sorption of peat humic acids to multi-walled carbon nanotubes, *Environ. Sci. Technol.*, 2011, 45, 9276-9283.

2. S. Madden, M. F. Hochella, T. P. Luxton, Insights for size-dependent reactivity of hematite nanomineral surfaces through Cu2+ sorption, *Geochim. Cosmochim. Acta.*, 2006, 70, 4095–4104.

3. S. Xu, A. H. Habib, S. H. Gee, Y. K. Hong, M. E. McHenry, Spin orientation, structure, morphology and magnetic properties of hematite nanoparticles, *J. App. Phy.* 2015, 117, 17A315.

4. S. Ghosh, N. R. Pradhan, H. Mashayekhi, Q. Zhang, B. Pan, B. Xing, Colloidal aggregation and structural assembly of aspect ratio variant goethite (α-FeOOH) with nC_{60} fullerene in environmental media, *Env. Pollut.*, 2016, 219, 1049-1059.

5. S. Ghosh, Z-Y. Wang, S. Kang, P. C. Bhowmik, B. Xing, Sorption and fractionation of a peat derived humic acid by kaolinite, montmorillonite, and goethite, *Pedosphere,* 2009, 19, 21–30.

6. Kasha, M., Characterization of electronic transitions in complex molecules, *Discuss. Faraday Soc.*, 1950, 9, 14−19.

7. N. J. Hestand, F. C. Spano, Expanded Theory of H- and J-molecular aggregates: The Effects of vibronic Coupling and Intermolecular Charge Transfer, *Chem. Rev.*, 2018, 118, 7069−7163.

8. B. Heyne, Self-assembly of organic dyes in supramolecular aggregates, *Photochem. Photobiol. Sci*., 2016, 15, 1103-1114.